Tectonics

RESEARCH ARTICLE

10.1029/2021TC006957

Key Points:

- We identify foreland intracratonic plateaus (FIPs) adjacent to fold-thrust belts of the Appalachian-Ouachita orogen
- FIPs are cratonic platform and foreland basin strata now elevated above deeply-eroded Paleozoic fold-thrust belts
- Greater resistance to erosion of FIPs than fold-thrust belts leads to topographic inversion during flexural unloading of the lithosphere

Correspondence to:

A. M. Anders,
amanders@illinois.edu

Citation:

Anders, A. M., Lai, J., & Marshak, S. (2022). Development of foreland intracratonic plateaus (Ozark Plateau and Appalachian Plateaus): A consequence of topographic inversion due to erosion of adjacent fold-thrust belts. *Tectonics*, *41*, e2021TC006957. https://doi.org/10.1029/2021TC006957

Received 22 JUN 2021
Accepted 11 MAR 2022

Author Contributions:

Conceptualization: Alison M. Anders, Jingtao Lai, Stephen Marshak
Investigation: Alison M. Anders, Jingtao Lai, Stephen Marshak
Methodology: Alison M. Anders, Jingtao Lai
Software: Alison M. Anders, Jingtao Lai
Visualization: Alison M. Anders, Jingtao Lai, Stephen Marshak
Writing – original draft: Alison M. Anders, Jingtao Lai, Stephen Marshak
Writing – review & editing: Alison M. Anders, Stephen Marshak

Development of Foreland Intracratonic Plateaus (Ozark Plateau and Appalachian Plateaus): A Consequence of Topographic Inversion Due To Erosion of Adjacent Fold-Thrust Belts

Alison M. Anders[1], Jingtao Lai[1,2], and Stephen Marshak[1]

[1]Department of Geology, University of Illinois at Urbana-Champaign, Urbana, IL, USA, [2]Now at Helmholtz Centre Potsdam, GFZ German Research Centre for Geosciences, Potsdam, Germany

Abstract Unlike well-known plateaus associated with Cenozoic orogens, the Appalachian and Ozark Plateaus of the eastern United States fringe the foreland side of a long inactive and deeply eroded orogen. These foreland intracratonic plateaus (FIPs), which are underlain by sub-horizontal cratonic-platform strata and, in places, foreland-basin strata, now lie 0.5–1.2 km above sea level, notably higher than adjacent fold-thrust belts. An escarpment lies at or near the boundary between the FIPs and the fold-thrust belts. Why did the topographic inversion leading to the development of the FIPs take place? To address this question, we built a numerical model, using *Landlab*, to simulate how topography evolves as foreland lithosphere flexes upward when post-tectonic erosion causes unloading. In this model, flat-lying cap-rock strata (sandstone and limestone) of the foreland have greater resistance to erosion than do the deformed, tilted, cleaved, and fractured strata of the fold-thrust belt, especially where the fold-thrust belt contains argillaceous facies. We tested the model by characterizing the development of the Ozark Plateau in the foreland of the Ouachita fold-thrust belt. Results demonstrate that regional isostatic uplift due to erosion, given reasonable differences in resistance to erosion between the fold-thrust belt and the foreland, can generate the observed topographic inversion and a distinct escarpment, yielding a plateau. This model may help explain the post-Paleozoic evolution of the Catskill Mountains, the Deep Valleys Province, and the Cumberland Plateau, highlands which border the Appalachian fold-thrust belt.

Plain Language Summary We identify plateaus in the eastern United States that did not become plateaus during mountain growth, but instead are the consequence of erosion after mountain building ceased. These plateaus share key features: (a) all fringe the Appalachian and Ouachita Mountain belts; (b) all incorporate the undeformed (flat-lying) sedimentary beds that had been deposited on continental crust; (c) all now lie at higher elevation than the remnants of the mountains which once towered above them; and (d) an escarpment defines the boundary between the plateau and the eroded mountain belt. To explain the development of these plateaus, we simulated erosion using a computer model. Our model takes into account the greater strength of flat-lying rock layers than the broken and tilted rock layers of a mountain belt. Because of the elastic behavior of the lithosphere, erosion of the mountain range results in uplift over a broad area that includes the nearby flat-lying sedimentary beds much like stepping off a trampoline leads to upward motion of a broad area of the trampoline's surface. As uplift happens, over tens of millions of years, erosion lowers the area of the mountain range relative to the area containing the flat-lying beds of sediment, producing a plateau.

1. Introduction and Statement of the Problem

The Earth's most intensively studied plateaus—the Tibetan Plateau, the Altiplano, and the Colorado Plateau—developed in Cenozoic orogens due to one or more of the following processes: crustal thickening, underplating, heating, lithospheric delamination, or mantle upwelling (e.g., Allmendinger et al., 1997; England & Houseman, 1998; Levander et al., 2011; Liu & Gurnis, 2010; Powell, 1986). Not all present-day plateaus lie within or adjacent to Cenozoic orogens. For example, plateaus of the eastern and southeastern United States lie on the foreland side of the Appalachian-Ouachita orogen, which ceased being a collisional orogen by the end of the Paleozoic. Crust underlying these plateaus consists of Precambrian crystalline basement overlain by a relatively thin cover of nearly flat-lying Phanerozoic cratonic-platform marine and fluvio-deltaic strata and, in places, overlying clastic strata derived from erosion of the neighboring orogen. Because of their geologic context, we name these regions foreland intracratonic plateaus (FIPs). FIPs include the distal part of foreland basins, which had formed in response to loading of the continental margin by fold-thrust belts. When orogeny ceased, the land surface of a region that is now a FIP was lower than that of the adjacent fold-thrust belt, for the area of the FIP was accumulating sediment eroded from the fold-thrust belt. Now, in contrast, the average elevation of a FIP sits higher than that of the adjacent, deeply-eroded fold-thrust belt, and an escarpment sloping toward the fold-thrust belt defining the hinterland edge of the FIP exists at or near the boundary between the FIP and the fold-thrust belt. Therefore, development of FIPs in the eastern United States represents a topographic inversion that took place after orogeny ceased in post-Paleozoic time.

The FIPs bordering the Appalachian Mountains include the Catskill Mountains of eastern New York (which borders the Hudson Valley fold-thrust belt; Marshak, 1986), the Deep Valleys Province of central Pennsylvania (which borders the Pennsylvania Valley-and-Ridge Province), and the Cumberland Plateau (which borders the fold-thrust belt of Tennessee; Figure 1). These three FIPs are the particularly high portions of the regional Appalachian Plateau. Another FIP, the Ozark Plateau (which forms the highlands of Arkansas and Missouri in the Midcontinent of the United States), lies just to the north of the Late Paleozoic Ouachita fold-thrust belt. The FIPs of the eastern United States range in area from 15,000 to 130,000 km^2, meaning that the largest has an area comparable to that of the Altiplano. Relative to the plateaus associated with Cenozoic Orogens, however, FIPs are lower. Specifically, high points of the Colorado Plateau are over 2 km, those of the Altiplano are over 3 km, and those of the Tibetan Plateau are over 4 km, whereas ridges rise to about 0.7 km in the Ozark Plateau, 0.9 km in the Cumberland Plateau, 1.0 km in the Deep Valleys Province, and 1.2 km in the Catskill Mountains (Figure 2). The landscape within FIPs also differs from that of plateaus in Cenozoic orogens in that the former have been dissected by dendritic drainage networks whereas the latter have mostly broad planar surfaces surrounded by even higher mountains. FIPs qualify as plateaus, physiographically, not because they are very high, flat surfaces, but rather because their ridge crests have comparable heights, and their land surface, overall, sits higher than that of surrounding regions.

What mechanism produced the FIPs of the eastern United States? Davis (1882) was among the first to discuss this issue when he pointed out that the flat-lying strata of the Catskill Mountains sit nearly a kilometer higher than the deformed strata of the Hudson Valley Fold-Thrust belt (Figure 3) and emphasized that this spatial configuration contrasted with that of modern orogens, such as the Alps or Andes, where deformed rocks of the fold-thrust belt underlie mountains that tower over the undeformed rocks of the foreland. We suggest that a FIP begins to rise primarily due to regional flexural isostatic uplift accompanying post-orogenic erosion of the adjacent fold-thrust belt, when the erosion rate in the fold-thrust belt starts to exceed the rate at which new loads (thrust sheets) are emplaced on the continental margin. This mechanism of uplift was quantified by Beaumont (1981), Beaumont et al. (1982), and Jamieson and Beaumont (1988), who emphasized that erosion of the once high topography of the fold-thrust belt induces upward vertical displacement of the relatively broad region, including the foreland basin, that had previously been flexurally downwarped due to the load of emplaced thrust sheets. (Other mechanisms of uplift that may have occurred in the eastern United States may have amplified the FIPs, as described later.) We hypothesize that the topographic inversion that delineates a FIP takes place simply because rocks of the fold-thrust belt are more easily eroded than are those in the distal (undeformed) foreland basin (Figure 4). Because of differential erosion, the undeformed part of the former foreland basin and the cratonic platform margin becomes higher than the fold-thrust belt. The contrast in erodibility between the fold-thrust belt and the undeformed foreland exists in part because of contrasts in lithology (fold-thrust belts of the Appalachian-Ouachita orogen contain a higher proportion of argillaceous flysch, while FIPs contain a higher proportion of limestone and sandstone), and in part because tectonic tilting, fracturing, faulting, and fabric formation weakens deformed rocks making them more susceptible to weathering, mass wasting, and fluvial erosion.

To test our hypothesis, we used the *Landlab* platform (Barnhart et al., 2020; Hobley et al., 2017), to develop a numerical landscape-evolution model of a FIP. Pazzaglia and Gardner (2000) carried out a similar study, using a different software platform, to explain the development of escarpments on the east side of the Appalachians. As input into the model, we employed basic geologic and topographic characteristics of the Ouachita fold-thrust belt and its adjacent foreland, the southern margin of the Ozark Plateau. In other words, we apply our model to the Ouachita-Ozark region as a test case, a region that Corrigan et al. (1998) suggested had undergone uplift and denudation in response to flexural uplift. Below, we set the stage for our model by outlining the geologic history of the Ouachita-Ozark region, by reviewing studies of eastern United States uplift, and by providing evidence

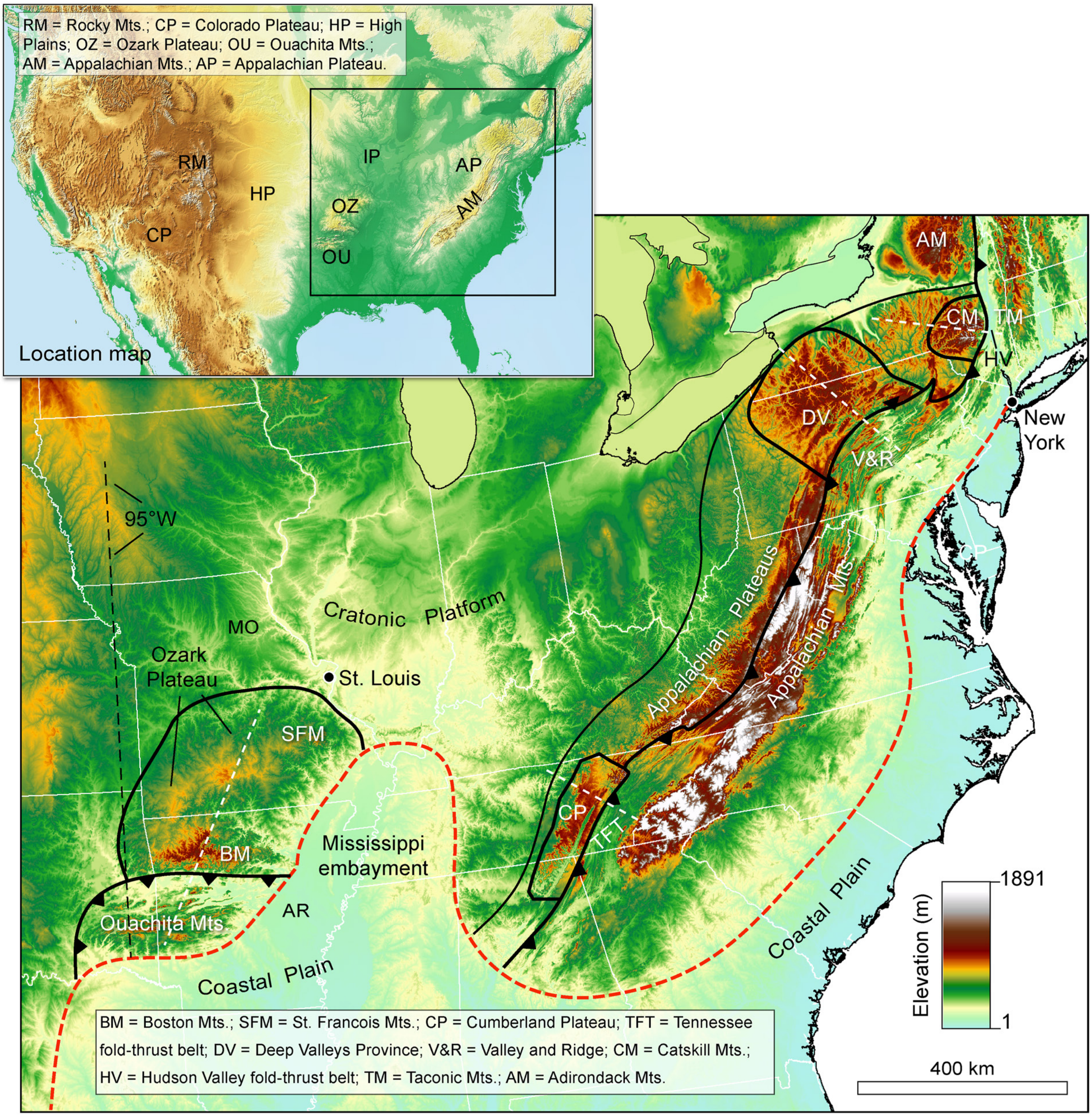

Figure 1. Location map shows the broad study area within North America. Foreland intracratonic plateaus (FIPs) of North America, outlined by black lines, include the Catskill Mountains (average elevation 560 m), the Deep Valleys Province (average elevation 520 m), the Cumberland Plateau (average elevation 395 m) and the Ozark Plateau (average elevation 290 m). Their adjacent fold-thrust belts, bounded by the toothed lines, are the Hudson Valley fold-thrust belt (average elevation 130 m), the Valley and Ridge (average elevation 290 m), the Tennessee fold-thrust belt (average elevation 270 m), and the Ouachita Mountains (average elevation 210 m). The FIPs are underlain by Paleozoic cratonic-platform strata and, in some places, by foreland-basin deposits. All border eroded Paleozoic fold-thrust belts. Topographic swath profiles across each FIP and fold-thrust belt, centered on the dashed white lines, are presented in Figure 2.

for systematic differences in the resistance to erosion between the undeformed strata of the foreland and the deformed strata of the fold-thrust belt. Then we describe our *Landlab* model and the results that come from it. Our model demonstrates that the topographic inversion that produces FIPs can be explained by differential erosion of flexurally uplifted lithosphere. The difference in elevation between a FIP and the adjacent fold-thrust belt does not require differential uplift (i.e., uplift of the FIP relative to the fold-thrust belt).

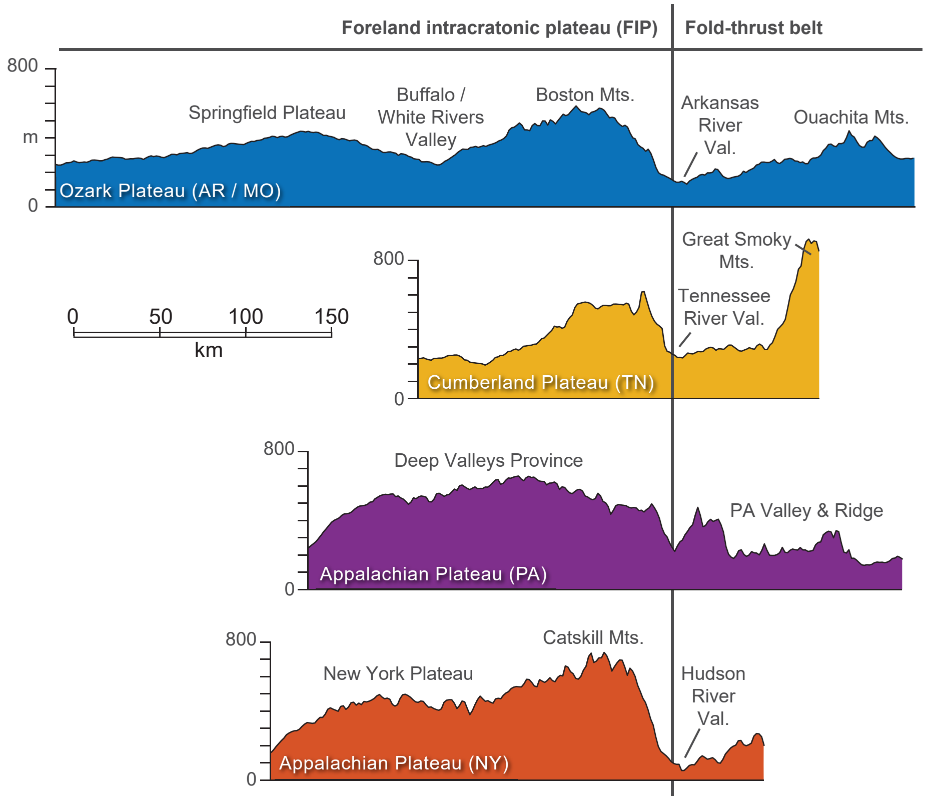

Figure 2. Mean elevations of topographic swaths across the FIPs and adjacent fold-thrust belts. The edges of the FIPs are aligned to show similarity of the transition from FIP to fold-thrust belt. Topography from the 1-km resolution GTOPO 30 DEM is averaged across 50-km wide swaths centered on lines approximately perpendicular the boundaries between FIPs and their associated fold-thrust belts (shown in Figure 1) using the SwathProfiler ArcGIS plug in tool (Pérez-Peña et al., 2017).

2. Background

2.1. Geologic History of the Ozark Plateau—Ouachita Orogen System

The model that we have developed to test our hypothesis incorporates characteristics of the Ouachita fold-thrust belt, the Arkoma foreland basin, and the Ozark Plateau (Figure 5). Traditionally, the Arkoma Basin has been depicted as the region between the Chocktaw and Ross Creek faults, the northernmost exposed major thrusts of the Ouachita fold-thrust belt, and the southern edge of the topographic Ozark Plateau. Notably, however, the Arkoma Basin has been mapped as extending further north in Oklahoma than it does in Arkansas, so at the end of deposition, the distal portion of the Arkoma Basin may have occurred over the southern Ozark Plateau, but was subsequently eroded. The hinterland edge of the basin occurred in a region that now lies within the Ouachita fold-thrust belt for, as is the case in many orogens, the fold-thrust belt eventually propagates into its own foreland basin. Also, basin strata between the Choctaw and Ross Creek faults and the southern margin of the Arkansas

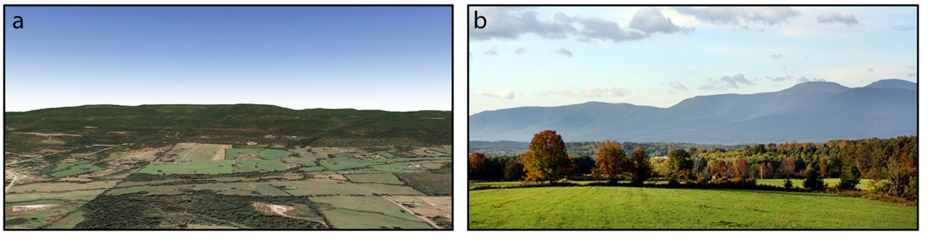

Figure 3. Landscapes of FIPs. (a) The southern margin of the Ozark Plateau, from Google Earth imagery; (b) The Catskill Mountains as viewed from the Hudson Valley.

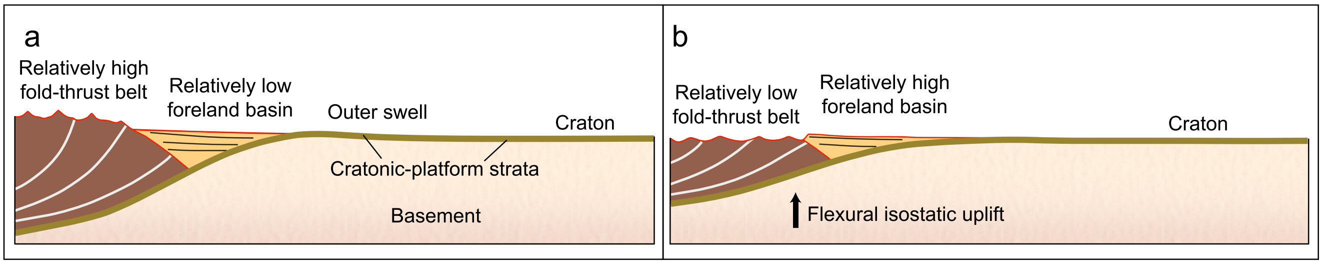

Figure 4. Cartoon cross-sections illustrating our hypothesis for the formation of FIPs. (a) The deformed strata of the Appalachian-Ouachita orogen in brown, which shed sediments (yellow) into a foreland basin during their growth. (b) The inversion of topography that develops because preferential erosion of the fold-thrust belt drives regional flexural isostatic uplift that raises the more resistant foreland basin of the craton edge.

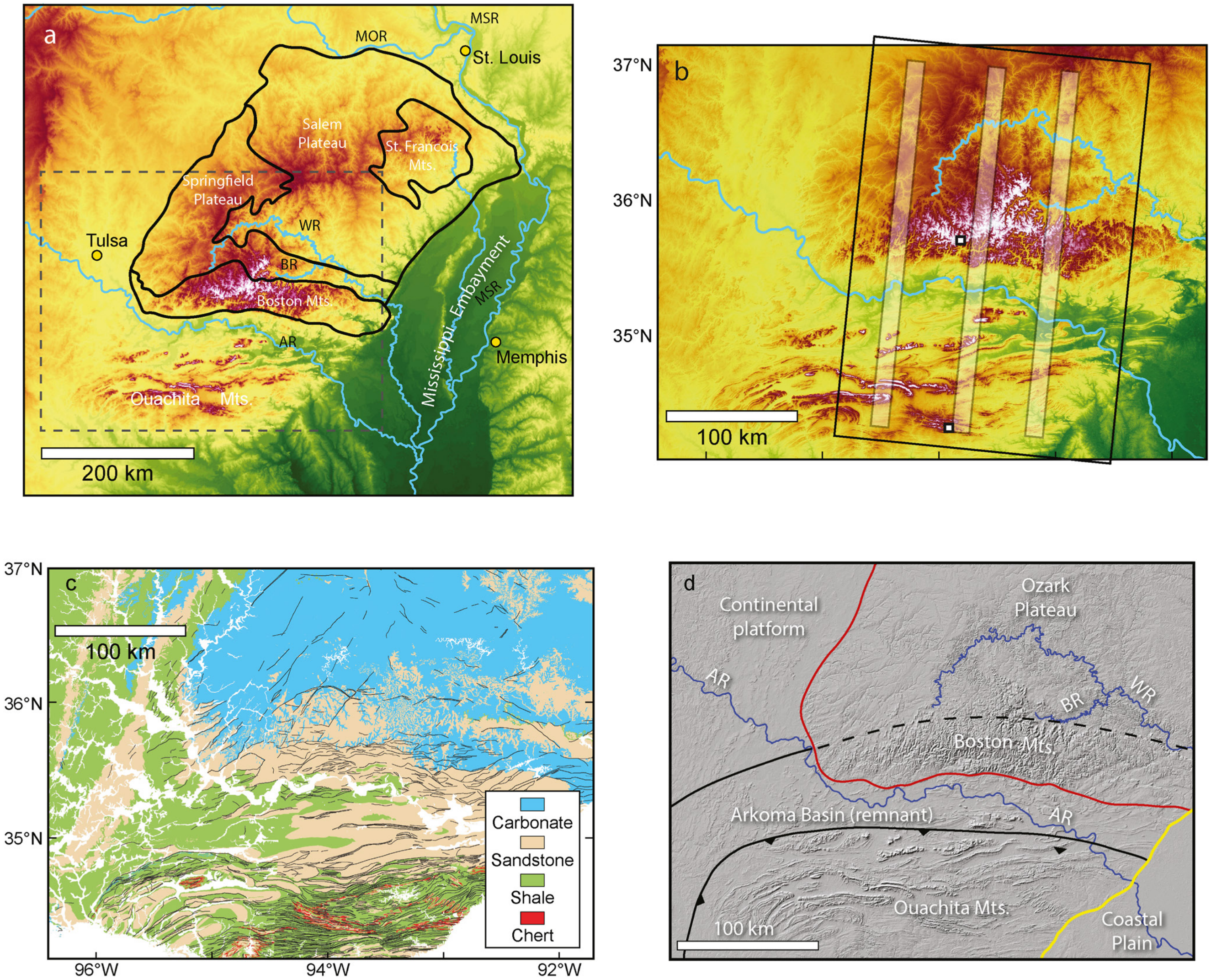

Figure 5. (a) Geography of the Ozark Plateau includes four physiographic subprovinces. The highest average elevations occur in the Boston Mountains (Figure 2), just north of the Arkansas River Valley and Ouachita Mountains. AR = Arkansas River; MSR = Mississippi River; MOR = Missouri River; BR = Buffalo River; WR = White River. Approximate area of figures b, c, and d shown as dashed gray box. (b) DEM of the Ozark Plateau and Ouachita Mountains. We model a domain of the size indicated by the black box. Small white boxes mark areas shown in Figure 7. Three topographic cross-sections indicated by shaded boxes are shown in Figures 9c–9e. (c) A simplified lithology map based on Horton et al. (2017). Note that shale dominates the Ouachita Mountains. The thin black lines are fault traces. (d) Approximate boundaries of the Arkoma Basin, Ouachita Mountains, and Ozark Plateau (modified from Northcutt & Campbell, 1995) overlain on a shaded relief map of topography. Dashed line indicates a speculative extrapolation of the Arkoma Basin, as it may have appeared prior to erosion.

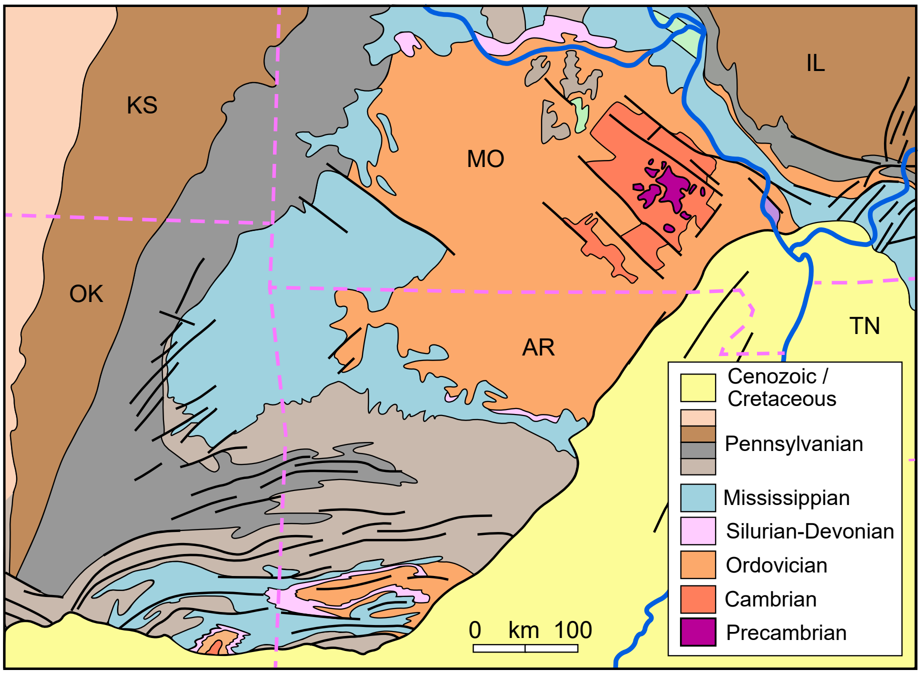

Figure 6. Simplified geological map of the Ozark Plateau and the Ouachita Mountains region. State boundaries shown as pink dashed lines. Note that older strata occur both in the southern Ouachitas and at the center of the St. Francois Mountains. The structural Ozark Dome has a somewhat rectilinear form, controlled by faulting.

River Valley, has been folded and fractured above blind thrusts (see cross sections in Arbenz, 1989a, 1989b, and Thomas, 2011). This deformation can be traced north to within 20–30 km south of the present escarpment that delineates the southern edge of the Ozark Plateau (Figure 5d; Arbenz, 2008; Hudson, pers. commun., 2022).

Physiographically, the Ozark Plateau has been divided into four subprovinces (e.g., Bretz, 1965), named from south to north (Figure 5b): (1) the Boston Mountains, a dissected ridge topped by Pennsylvanian sandstone; (2) the Springfield Plateau, topped by Mississippian Limestone; (3) the Salem Plateau, topped by Ordovician dolostone; and (4) the St. Francois Mountains, where Paleozoic strata taper out so that the Great Unconformity and the underlying basement of 1.47 Ga granite and rhyolite are exposed. The highest elevations of the Ozark Plateau occur in the Boston Mountains and in the St. Francois Mountains. The western edge of the Ozark Plateau gradually descends westward to lower elevations, while the eastern edge drops abruptly down to the Mississippi Embayment.

The region of our case study overlies what was, during much of the Paleozoic, the southern margin of North America. This margin initiated as a transform margin during Iapetan rifting (Thomas, 1976, 2011), and then evolved into a narrow passive-margin that lasted until the Carboniferous (e.g., Sutherland, 1988). The region to the north of the passive-margin was a cratonic platform that was undergoing differential epeirogenic movements to form regional basins and domes (e.g., Ham & Wilson, 1967; Marshak & van der Pluijm, 2021). The region that would become the Ozark Plateau developed, structurally, into the Ozark Dome, whose apex now occurs in the St. Francis Mountains. Strata dip gently away from the apex of the dome, so the pattern of contacts on geologic maps of the Ozark Plateau resembles a bullseye (Figure 6). The Ozark Dome's structure influences regional bedding dips as far south as the Arkansas River Valley, for in the southern Boston Mountains, strata dip at a few degrees southward. The dome area remained relatively shallow, or even emergent, at times when deposition was taking place in surrounding basins. Locally, sets of steeply-dipping faults cut through cover and basement rocks of the region. Displacement on these faults influenced local stratigraphy and bedding attitudes (e.g., Cox, 2009; Hudson, 2000; Marshak & Paulsen, 1996; McCracken, 1971; Nelson, 1995).

By the dawn of the Mississippian, plate convergence had initiated south of North America (present-day reference frame), and oceanic lithosphere was being consumed along a south-dipping subduction zone (e.g., Sutherland, 1988; Viele & Thomas, 1989). By Early Pennsylvanian, a thick turbidite succession had started to accumulate along the

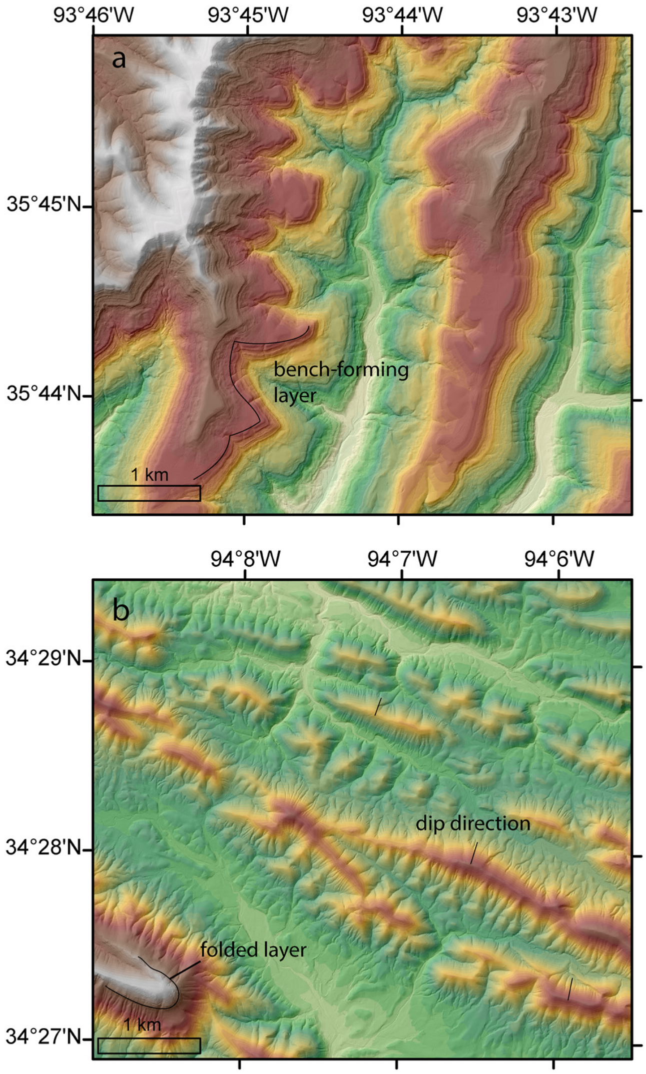

Figure 7. Detailed topography from the Boston Mountains and Ouachita Fold-thrust belt at locations indicated by white boxes in Figure 5b. Both images show 1-m resolution DEM from The National Map, using the same colorscale (elevations ranging from 300 to 725 m). (a) In the Boston Mountains, differential erosion of flat-lying layers produces horizontal benches and dendritic drainage patterns. The drainage divide in the upper left is asymmetric with steeper channels draining south to versus more gentle slopes toward the plateau interior. (b) In contrast, the topography of the Ouachita fold-thrust belt indicates the strong control of sloping units of variable hardness on both topography and drainage patterns. High elevations are held up by ridges of chert or novaculite. Trellis drainage had developed in softer rock between these hard units. Overall elevations are lower, due to the predominance of weak shale and slate. Resistant units are only able to sustain high elevations locally.

subduction zone (e.g., Houseknecht, 1983; Houseknecht et al., 2014). Eventually, an accretionary prism and the crust south of it collided with the passive margin, to produce the Ouachita fold-thrust belt (e.g., Arbenz, 2008; Viele & Thomas, 1989). Growth of the fold-thrust belt emplaced thrust sheets on the southern margin of North America, and the resulting load caused flexural downwarping of the margin (cf. Beaumont, 1981; DeCelles & Giles, 1996; Price, 1973), along with syn-depositional normal faults (e.g., Houseknecht et al., 2014; Sutherland, 1988; Viele, 1973). One of these faults, the Mulberry Fault, emerges along the southern edge of the Boston Mountains, and delineates the boundary between horizontal strata of the Boston Mountains, and south-dipping strata of the northern Arkansas Valley (Al Asadi et al., 2017; Arbenz, 1989b; Haley et al., 1993; Houseknecht, 1986; Long, 2005). Downwarping established the Arkoma Basin as peripheral foreland basin (i.e., a foreland basin developed on the continental margin of the downgoing plate; e.g., DeCelles, 2012). By Middle Pennsylvanian, the hinterland of the fold-thrust belt had may have become emergent and sediments derived from the fold-thrust belt contributed to the rapid filling of the Arkoma Basin. As noted earlier, as the Ouachita fold-thrust belt grew, thrusting propagated progressively northward into the Arkoma Basin, so blind thrusting propagated to within about 20 km of the southern edge of the Boston Mountains, and overlying strata deformed into folds. Coeval slip on reactivated steep faults took place within the Ozark Plateau (e.g., Cox, 2009; Hudson, 2000; Marshak & Paulsen, 1996; McCracken, 1971; Nelson, 1995).

2.2. Contrasts in Resistance to Erosion Between the Ouachitas and the Ozark Plateau

The geomorphology of the Boston Mountains differs markedly from that of the Ouachita fold-thrust belt. Nearly flat-lying strata of the former have eroded to produce distinct benches in the landscape cut by dendritic drainage (Figure 7a). In contrast, trellis drainage networks occur in the latter, for narrow bands of resistant novaculite or chert hold up narrow ridges, separated by valleys underlain by weak argillaceous strata (Figure 7b). We emphasize that the structural and lithological differences between these regions not only yields differences in drainage network morphology, but also causes a systematic difference in regional resistance to erosion.

Rock hardness provides one control on rock erodibility (e.g., Goode & Wohl, 2010; Lamb et al., 2015; Sklar & Dietrich, 2001). Previous researchers have reported Schmidt hammer rebound values (R) (Swanson, 2016; Thaler & Covington, 2016) and digital Rockschmidt hammer velocity values (Q) (Keen-Zebert et al., 2017; Peppers, 2015) for Ordovician-Pennsylvanian sedimentary units in the Boston Mountains and Ouachitas. Rebound values can be converted to velocity values, allowing direct comparison of these two types of measurements (Winkler & Matthews, 2014). Measurements from this region indicate sandstone, limestone and dolostone (R value equivalents of 37–62) are harder than shale (R value equivalents of 4–27). Based on the empirical relationship between R-values and tensile strength presented by Hosseini and Shirin (2015) we estimate that sandstone, limestone and dolostone have a tensile strength of ~20 MPa, and that shale has a tensile strength of <4 MPa. The relationship between erosion rate and tensile strength, as determined by Sklar and Dietrich (2001), indicates that erosion rates for shale are likely 25× that of sandstone, dolostone and limestone in this region, for a given river slope and discharge. The greater prevalence of shale (slate) in the Ouachitas, relative to the limestone, dolostone and sandstone that dominates in the Boston Mountains (Figure 5c), indicates that resistance to erosion in the Ouachitas overall is likely significantly less than that in the Boston Mountains, regardless of contrasts in degree of deformation.

In the Ozark-Ouachita region, intact rock hardness is not the only possible control on erosional resistance—contrasts in degree of deformation also affect resistance. Specifically, the frequency and character of joints, fractures, and cleavage planes in rocks correlates with rock strength, for the presence of these weak partings allows fragmentation to take place more easily, so rates of mass wasting, as well as fluvial and glacial plucking, correlate with the presence of these structures (e.g., Marshall & Roering, 2014; Miller, 1990; Nasseri et al., 1997; Oskin et al., 2014; Selby, 1982; Wylie & Mah, 2001). The dip angle of fractures and bedding planes also influences erosion rates (e.g., Dühnforth et al., 2010; Hancock et al., 1998; Hooyer et al., 2012; Kelly et al., 2014; Krabbendam & Glasser, 2011; Scott & Wohl, 2019). Notably, Baker (2013) documented a strong relationship between the dip of bedding planes or joint surfaces and observed failure of bedrock outcrops of the Arkansas Valley. She found failure becoming nearly ubiquitous above a critical dip angle of 26 for sandstone and 7 for shale. Clearly, tilting of bedding due to faulting and folding facilitates hillslope erosion in this region. Because bed tilt (due to faulting and folding), cleavage development, and fracture density in the Ouachitas and Arkansas Valley exceeds that of the Boston Mountains, the latter region is more resistant to erosion (Figure 5c). Given that Boston Mountains are also more resistant to erosion because of lithology, we conclude that our proposal that the foreland region now within the Ozark Plateau eroded less rapidly than the fold-thrust belt of the Ouachitas and Arkansas Valley is quite reasonable.

2.3. Previous Studies of Uplift and Exhumation in Eastern North America

Differential erosion cannot take place in the absence of uplift. Many lines of evidence indicate that uplift and exhumation occurred in the eastern half of the United States after the late Paleozoic collisions that formed the Appalachian-Ouachita orogen. Initial evidence comes from study of paleotemperature indicators. These suggest that Paleozoic strata now exposed at the Earth's surface in the foreland of the orogen were once significantly hotter (>110°C), an observation that has led some researchers to suggest that the strata were once buried more deeply and subsequently underwent exhumation (e.g., Levine, 1986). The amount of maximum burial remains controversial, however, because of uncertainty over the possibility that syn-tectonic migration of hot groundwater contributed to the elevated temperatures indicated by paleothermometers (Bethke & Marshak, 1990; Mariño et al., 2015; Oliver, 1986).

More recently, thermochronologic studies also have constrained the amount as well as timing of exhumation. For example, apatite fission-track studies indicate that rocks now at the surface in the eastern platform and adjacent foreland basins underwent exhumation of 2–5 km subsequent to maximum heating (Crowley, 1991; Miller & Duddy, 1989), with exhumation of the Catskill Mountains region of New York occurring in the Early Cretaceous, and strata now exposed elsewhere in the Appalachian Plateau beginning to undergo exhumation in the Late Triassic. Roden and Miller (1989) suggest that a pulse of cooling also occurred in the Middle Jurassic to Early Cretaceous. Thermal modeling, in conjunction with apatite fission-track dating led Blackmer et al. (1994) to propose that the foreland basin in Pennsylvania underwent a rapid episode of exhumation in the Late Permian through Early Jurassic, a slow episode during the remainder of the Mesozoic; and a rapid episode in the Miocene to present. Fission-track dating of Precambrian basement and Cambrian sedimentary rocks indicates that the St. Francis Mountains underwent uplift and cooling in the Late Cretaceous (Arne et al., 1990). Maximum thermal maturity in the foreland basin of the Ouachitas was achieved prior to Cretaceous and cooling to less than 80°–90° took place in Middle Cretaceous, suggesting exhumation rates of a few tens of meters per million years (Arne, 1992; Corrigan et al., 1998). (U/Th)/He studies and associated thermal modeling suggest that about 3 km of post-Pennsylvanian strata were stripped from the central Midcontinent (Illinois Basin) during the Mesozoic and Cenozoic (Lovell, 2017), and that exhumation of broad regions of the craton took place in Late Paleozoic to Early Mesozoic time 350–250 Ma (Flowers et al., 2012; Zhang et al., 2012). Interpretation of AFT and (U/Th)/He data from the Ozark Plateau point to Late Jurassic and Early Cretaceous (225–150 Ma) exhumation events (DeLucia et al., 2018).

Thermochronologic and geomorphological evidence hints that slow uplift has continued into the Cenozoic. For example, Corrigan et al. (1988) suggest that the Ozark-Ouachita region had been covered by about 1 km of Cretaceous-Paleogene strata which has since been eroded. Brown (2005) suggested that uplift continued into the Cenozoic, based on fission-track dating of detrital apatite from cores from Missouri. Beeson et al. (2017) showed that drainage networks of the Ozark Plateau have not reached an equilibrium in which erosion rates are spatially uniform and stream profiles have uniform concavity. They came to this conclusion by comparing erosion rates on streams throughout the Plateau, by documenting the asymmetry of drainage divides, and by finding morphological evidence of stream capture. The disequilibrium demonstrated by Beeson et al. (2017) could indicate that uplift rates have changed more quickly than the response time of the river network, which they argue may be as long as hundreds of millions of years. The presence of bedrock-incising streams, characteristic of young landscapes, also suggests disequilibrium. Cosmogenic Be-10 ages and denudation rates suggest that topography has been rejuvenated in the Appalachians (Miller et al., 2013), and in the Ozarks (Reminga et al., 2016; J. Weber, pers. commun., 2021).

Debate continues on the causes of widespread post-Paleozoic uplift in eastern United States. Uplift has been attributed to Mesozoic rifting, either associated with rift-related thinning of lithospheric mantle, thickening of the continental crust by basaltic underplating, or lateral heating (e.g., Beaumont et al., 1982; Hrubcová et al., 2017; Nyblade & Sleep, 2003; White & McKenzie, 1989). Flowers et al. (2012), proposed that uplift is a manifestation of dynamic topography caused by upwelling after Pangaea amalgamation. The implications of dynamic topography on epeirogenic movements of eastern North America have also been explored by Moucha et al. (2008) and Liu (2014, 2015). Some authors have attributed vertical displacements in the midcontinent and eastern United States to mantle hotspots. For example, Crough (1981) used this approach to explain uplift in northeastern states. Cox and Van Arsdale (2002) present evidence for hot-spot activity in the vicinity of the Ozark Plateau, implying that lithospheric heating-related uplift also happened there. Chu et al. (2013), and Lin et al. (2017), suggested that hot spots localized Cenozoic tectonic activity in the Ozark Plateau and Mississippi Embayment. It has also been proposed that uplift has occurred in response to sustained slow erosion (Matmon et al., 2003; Spotila et al., 2004), to mantle hydration (van der Lee et al., 2008), to mantle convection following delamination (Byrnes et al., 2019; Murphy & Egbert, 2017), and to influx of warm mantle after North America has passed over a subducted slab of the Farallon plate (Miller et al., 2013). Hu et al. (2018) suggest that uplift of cratons happens during the supercontinent cycle and represents an isostatic response to delamination. Some authors have suggested that continuing uplift may be a cause or consequence of seismic activity on continental-interior faults (e.g., Cox, 1988; McKeown et al., 1988; Purser & Van Arsdale, 1998; Thompson Jobe et al., 2020; Van Arsdale et al., 1995; Yang et al., 2014), or may be related to changes in eustatic sea level (e.g., Corrigan et al., 1998).

3. Hypothesis and Methods

3.1. FIPs and Their Formation

A FIP is a region of relatively elevated land underlain by nearly flat-lying, undeformed strata that lies on the craton side of a fold-thrust belt. Examples occur bordering Paleozoic fold-thrust belts of the Appalachian-Ouachita orogen in the eastern United States. In each case, the escarpment that delineates the hinterland side of the FIP formed near the boundary between the undeformed foreland and the fold-thrust belt. Why did FIPs of the eastern United States form? Specifically, does the high elevation of FIPs relative to adjacent fold-thrust belts—an elevation difference that represents a topographic inversion between the orogen and its foreland—develop due to: (1) Cenozoic faulting; (2) Cenozoic dynamic process that caused the foreland to rise independently of the fold-thrust belt: or (3) differential post-Paleozoic erosion?

We hypothesis that differential post-Paleozoic erosion acting on the region that underwent post-orogenic flexural uplift of Appalachian-Ouachita orogen and its foreland can produce FIPs without requiring other mechanisms. This differential erosion takes place because the undeformed less-argillaceous strata of the foreland are more resistant overall than are the deformed more-argillaceous strata of the adjacent fold-thrust belt. So, even though the fold-thrust belt was initially higher than the foreland, and experiences greater flexural uplift than the foreland, the foreland ends up being higher than the fold thrust belt after tens of millions of years. An erosional escarpment defines the orogen-side edge of the FIP. This boundary may have initiated at the boundary between relatively undeformed strata of the foreland basin, and the deformed strata of the fold-belt and defines the hinterland plateau edge, but subsequently, has undergone cliff retreat so that, in the case of the Ozark Plateau it lies as much as 20–30 km from the contact, and in the case of the Catskill Mountains, lies about 6 km to the foreland of the thrust front. (The greater distance between the thrust front and the escarpment in the Ozarks may reflect the presence of normal faulting and associated tilting of strata in the Arkansas Valley; Hudson, pers. commun., 2022.) Put another way, after the cessation of convergent orogeny, a topographic inversion develops between the fold-thrust belt and its foreland, and then migrates by cliff retreat toward the foreland (Figure 4). If differential erosion is the main control on the present elevation difference between FIPs and the adjacent fold-thrust belt, then regional flexural uplift can yield observed present-day elevation—the region of the FIP did not undergo differential tectonic uplift relative to the fold-thrust belt. Corrigan et al. (1998) made a similar suggestion, based on their interpretation of apatite fission-track data, which showed that rates of exhumation in the Ouachitas were greater than those in the foreland, as would be expected if uplift was driven by the flexural response to unloading. They also pointed out that the same phenomenon occurs to the west of the Ouachitas, where other uplifts (e.g., the Llano uplift) lie to the foreland of the fold-thrust belt.

3.2. A *Landlab* Numerical Model

To test our hypothesis, we developed a numerical model of topographic evolution to show how the surface elevation of a fold-thrust belt and the adjacent foreland develops due to fluvial erosion, if erosion causes the lithosphere to undergo flexural uplift in response to unloading. To constrain the model, we input characteristics of the Ozark Plateau-Ouachita fold-thrust belt region. Initially, the land surface of the model includes a higher-elevation fold-thrust belt and lower-elevation foreland. The "fold-thrust belt" is underlain by deformed strata and the "foreland" represents the distal, undeformed part of a foreland basin and/or a cratonic platform. (Deformed rocks that were ruptured and tilted not by thrusting, but rather by normal faulting and tilting, are lumped together with rocks that were disrupted by thrusting.)

Our numerical model (available at https://github.com/laijingtao/ozarks/) was built using the *Landlab (v. 1.5.1)* open-source platform (Barnhart et al., 2020; Hobley et al., 2017). Our model incorporates a well-established fluvial-erosion law:

$$E = K_{\mathrm{sp}} A^m S^n, \tag{1}$$

where fluvial erosion rate, E, is a function of the drainage area, A, and slope, S. The coefficient, K_{sp}, represents resistance to erosion. Therefore, our model uses a higher value of K_{sp} to represent the erodibility of deformed rocks in the fold-thrust belt than to represent erodibility of flat-lying strata in the undeformed foreland.

Based on measured rock hardness, lithology, bedding dip, and fault density, as described in Section 2.2, we conservatively suggest that K_{sp} of different regions in the model differ by at least a factor of 2–10. So, we fix the fold-thrust belt value of K_{sp} at $5\mathrm{e}^{-7}\ \mathrm{yr}^{-1}$ and vary the foreland K_{sp} from $5\mathrm{e}^{-8}$ to $5\mathrm{e}^{-7}\ \mathrm{yr}^{-1}$. Varying K_{sp} for the foreland allowed us to explore how changes in relative erosion resistance affects topography. Of course, it is difficult to establish the exact contrast between the resistance to erosion of the fold-thrust belt relative to the foreland, because other factors (e.g., slope, drainage area, climate, and uplift rate) also influence erosion rates, and these factors change through time. The exponents m and n are constants which we fix at 0.5 and 1, respectively—this choice of m and n has been found to be most consistent with fluvial erosion in the absence of significant karst (e.g., Anthony & Granger, 2007). The D8 algorithm controls routing of water flow across the model so that water flow follows the line of the steepest descent (O'Callaghan & Mark, 1984). In our model, hillslope erosional processes are modeled as a linear diffusion process using the *LinearDiffuser* component in *Landlab* (e.g., Culling, 1963). The value of diffusivity is set to scale with K_{sp} and it is 500 times greater than the value of K_{sp}. This scaling relationship ensures that the fold-thrust belt has higher values of diffusivity than does the foreland.

Our model combines erosion equations with standard equations representing flexural isostasy. Response of the lithosphere to erosional unloading is idealized as flexure of a one-dimensional beam, with a uniform elastic thickness, oriented perpendicular to the range front (e.g., Turcotte & Schubert, 2002). Significantly, for the range of elastic thicknesses appropriate for a cratonic setting (i.e., ∼10 s of km), the flexural wavelength is broader than the fold-thrust belt. To simplify our calculations, we assume that flexure dominates over time scales of tens of millions of years. This simplification is reasonable given the cold temperatures and thick effective elastic thickness of cratonic lithosphere. Real lithosphere would exhibit some viscoelastic behavior over this time period (Waschbusch & Royden, 1992), and such behavior could influence the dimensions of the region undergoing uplift, as well as the magnitude of uplift, as demonstrated by Ruetenik and Moucha (2021) for a passive margin escarpment setting, and by Beaumont (1981) and Quinlan and Beaumont (1984) for the foreland of the Canadian Rockies. But this change would not affect the overall pattern of topography. Our model does not include spatially or temporally discrete uplift events, such as those that may have affected the eastern Appalachians (see McKeon et al., 2014).

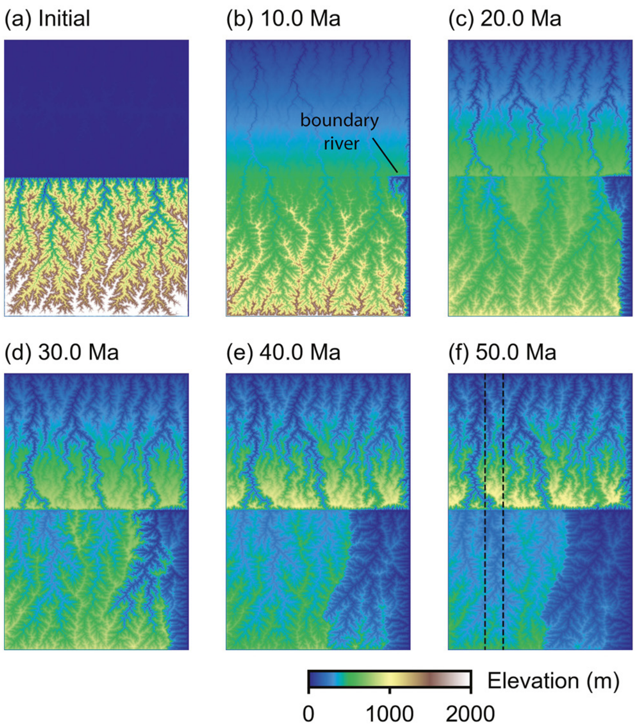

Figure 8. Modeled evolution of topography over 50 million years. (a) The initial condition includes a high fold-thrust belt and a nearly flat, low-elevation foreland basin. The fold-thrust belt is five times easier to erode than the foreland basin. Water and sediment exit the domain on the top and along the right side. Flexural uplift driven by unloading brings up the foreland basin and an escarpment develops along the basin edge. A boundary river propagates, beheading streams and facilitating further growth of the foreland plateau. Dashed lines in (f) show the location of topographic swath profiles compared to real topography in Figure 9.

In detail, the model consists a rectangular "map area," with the top of the map area (as viewed on a page) designated as the north direction, to simplify discussion. The map area contains two equal-sized "domains"—the northern one (called the "foreland domain") represents the region of undeformed strata that becomes the Boston Mountains of the Ozark Plateau, and the southern one (called the "fold-thrust belt domain") represents the Ouachita fold-thrust belt (Figure 5b)—the domains join along an east-west-trending straight line. Each 150 km (N-S) by 200 km (E-W) domain is subdivided into a grid squares representing 1 km^2. The initial conditions of the model represent topography at the end of the Ouachita collisional orogeny (Figure 8a). Initial topography of the fold-thrust belt domain was produced by simulating fluvial erosion using Equation 1, with one open boundary on the north side of the domain, uniform and constant uplift, and a fixed K_{sp} of 5e^{-7} yr^{-1} until a steady-state topography was achieved. Consequently, the land surface of this domain, overall, slopes moderately toward the foreland, and the surface contains numerous north-flowing channels. Initial topography of the foreland domain represents a steady-state landscape formed by fluvial erosion under conditions of uniform and constant (but very slow) uplift with an open boundary to the north. (This configuration is justified by making a comparison to the present-day topography of the Canadian Rockies in southern Alberta, where the land surface of both the fold-belt and the foreland basin slope, overall, toward the craton interior.) When a model run starts, the maximum elevation of the northern domain, at its boundary with the southern domain, is 20 m. The foreland domain slopes very gently toward the north and contains subtle channels draining to the north.

After establishment of initial conditions, no independent uplift is imposed on the map area. Instead, uplift occurs only as a flexural response to erosion. The two domains are connected across the boundary between them, so the flexural response is that of a continuous piece of lithosphere (i.e., a beam oriented N-S)—the domains differ from each other only in their resistance to erosion at the surface, and their initial land elevation. Starting from the initial condition, a given model run simulates the post-orogenic evolution over a duration of 50 million years, by calculating the elevation for each 1 km^2 grid square on the map after each 1,000-year timestep. We average the amount of erosion along the beam and then use the *gFlex* component in *Landlab* to compute flexural response (Wickert, 2016). Notably, one end of the beam is located at the southern edge of the map area, while the other end extends beyond the northern end of the map area, so that the total length of the beam is 700 km, a distance twice as long as typical flexural wavelength for continental lithosphere. Consequently, we can use the "0Displacement-0Slope" condition for the north end of the beam. In the model, we utilize the "mirror" boundary condition in *gFlex*, in which the southern edge of the map area represents a plane of mirror symmetry. As a model progresses, material eroded by streams travels out of the map area through the north and east boundaries while the other boundaries (south and west) are closed. These boundary conditions simulate the presence of a major river on the east of the Ozark Plateau, and the lack of a major river on the west.

We ran two groups of models. In the first group, we vary the contrast in resistance to erosion while holding the elastic thickness constant at a moderate value. In the second group, we fix the contrast in resistance to erosion at a factor of 5 and model a range of values for elastic thickness of the lithosphere. Below, we describe the observed evolution of topography in our models, and we compare our modeled topography to observed topographic cross-sections across the present-day Ouachita fold-thrust belt and Ozark Plateau (Figure 5b).

4. Results

As a model run begins, fluvial erosion deepens the pre-existing channels in the fold-thrust belt domain (Figure 8b). This incision drives uplift of the entire map area. Consequently, the foreland domain rises above base level so that the subtle channels draining to the north in the initial condition deepen. New channels initiate and propagate

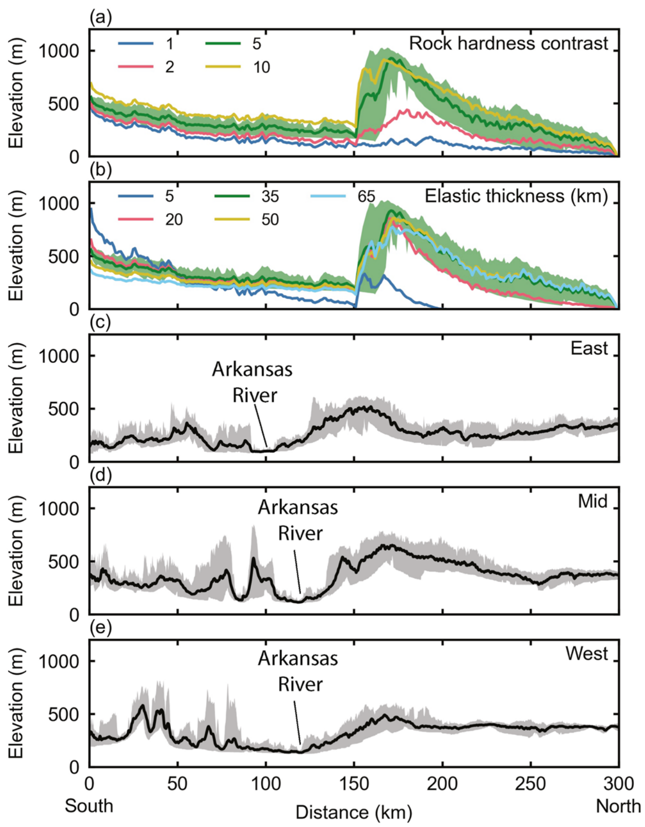

Figure 9. (a) and (b) are topographic profiles taken along the swath shown in Figure 8f. The mean topography is marked with a green line with the maximum and minimum topography shown as the green envelope. (a) The average topography of profile for varying rock hardness contrasts with fixed elastic thickness of 35 km in colored lines. A contrast of only 2, shown in red, produces a high foreland basin and a basin-edge escarpment. (b) The average topography of profile for a range of elastic thicknesses with a fixed rock hardness contrast of 5. The topography is relatively insensitive to elastic thickness for values from 20 to 65 km. An elastic thickness of 5 km, shown in dark blue, produces a high basin and escarpment, but maintains maximal topography in the center of the fold-thrust belt where uplift is focused. (c–e) The mean topography in black and the envelope of minimum and maximum topography in gray for the swaths shown in Figure 5b.

along the eastern boundary of the entire map area, and an east-flowing "boundary river" develops at the boundary between the two domains. As this river begins to capture drainage area from the fold-thrust belt domain, it slowly extends headward (for a total of about 50 km during the model run; Figures 8c–8f). A wave of incision initiates at the northern edge of the foreland domain and propagates southward so that channels of this domain eventually connect to those draining to the north off of the fold-thrust belt domain. Meanwhile, the boundary river incises more deeply and a series of short, parallel channels, draining to the south, form along the southern edge of the foreland domain. As the boundary river undergoes headward erosion, it also captures channels draining the fold-thrust belt domain, driving a wave of incision in their drainage basins.

As the drainage networks evolve, flexural uplift takes place over the entire map area, but more happens in the fold-thrust domain than in the foreland domain. During uplift, the contrast in resistance to erosion causes the northern toe of the fold-thrust belt domain to become lower in elevation than the adjacent margin of the foreland domain. Eventually, an escarpment forms along the boundary between the two domains on the north side of the boundary river. An east-west-trending drainage divide develops near the southern edge of foreland domain. Note that streams to the south of this divide are shorter and steeper than those to the north. As a model progresses, the fold-thrust belt domain continues to erode at a faster rate than does the foreland domain, so the drainage divide at the top of the escarpment becomes the highest land surface of the map area. Even where early-formed rivers still cut across the fold-thrust belt/foreland boundary a discontinuity forms at the junction of the fold-thrust belt domain and the foreland domain, so that the escarpment becomes a prominent landform across the entire map area (Figure 8f).

The qualitative evolution of the landscape including the formation of a foreland plateau is robust across a range of values for the elastic thickness of the lithosphere and for a range of different degrees of contrast in rock hardness between the fold-thrust belt and the foreland, as illustrated by topographic profiles (Figure 9). A factor of two difference is sufficient to produce an escarpment at the boundary between the two domains, with the land surface just north of this escarpment rising to an elevation greater than that of most of the fold-thrust belt (Figure 9a). For a fixed rock-hardness contrast, the average N-S topographic profile across the map area of our model is relatively insensitive to elastic thickness for values of 20–65 km, which are typical of continental lithosphere (Figure 9b). An elastic thickness of only 5 km still produces enough uplift of the foreland domain to create an escarpment and increase the elevation of the southern portion of the foreland domain by several hundred meters. In this case, the southern edge of the fold-thrust belt domain remains relatively high, because the horizontal length-scale of the flexure is much shorter and focuses uplift much more strongly within the fold-thrust belt than happens when the elastic thickness is greater.

5. Discussion

5.1. Comparing the Model to Reality

We chose the spatial scale, rock hardness contrast, and flexural thickness in our model to approximate the topographic evolution of the Ozark Plateau and Ouachita Fold-thrust belt, so the test of our model comes from comparing profiles produced by the model to real profiles across the Ouachita-Ozark region. As illustrated by Figure 9, after 50 Myr of topographic evolution, the modeled topography is indeed similar in overall shape and scale to observed profiles of present-day topography in that the Ouachita fold-thrust belt slopes, overall, toward the Arkansas River, while the Boston Mountains have a fairly steep southern margin, and gentler northern slope.

Also, the average elevation of the modeled fold thrust-belt decreases from approximately 400 m at the south edge of the map area of to 200 m at the northern edge, and the modeled foreland rises elevation of ~1,000 m just north of a boundary river. This compares favorably with change from an elevation of about 470 m of most ridge crests in the Ouachitas down to 170 m in the Arkansas Valley, and a rise to 640 m at the top of the escarpment between the Arkansas River Valley and the Boston Mountains.

There are differences, however, between the modeled topography and real topography. Specifically: (1) while both the model and observed topography have an escarpment facing the fold-thrust belt, the steepness of the actual escarpment on the south flank of the real Boston Mountains varies along significantly along strike while that in our model does not; (2) cliffs composed of resistant cap rocks fringe the northern edge of the real Boston Mountains, but do not exist in our modeled topography; (3) distinct ridges of resistant strata (some higher than the Boston Mountains) exist in the real Ouachita Mountains, where they control a trellis drainage pattern, but such ridges do not exist in our model and drainage all flows northward. The difference between model results and reality probably reflect the fact that the material properties of bedrock of the real landscapes are much more heterogeneous than those of the substrate in our model, while our model simplifies calculations by assuming that rock is homogeneous within a domain. Significantly, though, while resistant beds do hold up ridges in the Ouachitas, their steep dips mean that they cover a relatively small area overall, and therefore do not control the overall elevation of the Ouachitas. In contrast, flat-lying beds of resistant caprock do control plateau elevations in the Ozark Plateau.

Our model also does not account for variations in erosion rates in space and time across this region throughout the Mesozoic and Cenozoic due to climatic variability, changes in rock resistance during progressive unroofing, changes of base level and discharge of in the Mississippi, Arkansas, and Missouri Rivers which drain the region, and cliff retreat that happened once the edge of the FIP has been established. In particular, positive feedbacks may exist, in that once the major river systems are established, they control erosion of the Ozark Plateau. Because of the lack of constraint that we have on observed erosion rates, the timescale of evolution of the drainage network in our model is somewhat arbitrary—it would vary significantly with the choice of magnitude for the resistance to erosion and would be affected by the time scale of viscous flow in the lithosphere. Therefore, we cannot infer that our model indicates that the present topography represents specifically 50 million years of differential erosion. Furthermore, in the model, the boundary river extends in the headward direction unrealistically slowly and remains a minor drainage, perhaps because unlike the real Arkansas River, it does not carry water entering the map area from the west.

5.2. Implications and Remaining Challenges

When active tectonic thickening of a fold-thrust belt ceases, and erosion begins to permanently decrease the load imposed by the weight of the thrust wedge on the edge of the continental lithosphere, flexural uplift of both the fold-thrust belt and the adjacent foreland begins. Our modeling demonstrates that if, during this process, the fold-thrust belt exhumes by at least twice the rate of the undeformed foreland, a topographic inversion develops over a time scale of tens of millions of years. Specifically, the fold-thrust belt becomes lower, overall, than the undeformed foreland—in some cases, foreland basin strata that had been derived from the fold-thrust belt ends up being topographically higher than the fold-thrust belt. A distinct escarpment develops between the former and the latter, defining the hinterland edge of a FIP. Consequently, the existence of a FIP does not require that the foreland be uplifted independently of the fold-thrust belt. We are not aware of any distinct FIPs outside of eastern North America. In younger ranges, such as the Canadian Rockies, erosion of the fold-thrust belt has led to flexural uplift of the foreland, but not yet to topographic inversion (cf. Beaumont, 1981). In order for a FIP to become a prominent feature it needs to develop over long timescales in the absence of other landscape reshaping processes such as continental glaciation, flood basalt emplacement, and rift basin development. We suggest that these conditions have generally not been met outside of the broad Appalachian-Ouachita system in eastern North America.

While the topography of a FIP can be modeled assuming only flexural rebound due to erosion as a cause of uplift, we do not mean to imply that only flexure has affected the region. Other uplift drivers, described earlier, may certainly influence the overall uplift of the eastern United States, and could serve to amplify the topography that develops due to flexural uplift and differential erosion. For example, if the thermal consequences of rifting or upwelling of the asthenosphere were to cause regional-scale uplift, exhumation overall may be greater or have lasted longer, and FIPs may be higher than they would have been due to flexural uplift alone.

Our work draws attention to two important questions that we have not addressed with our models. First, why does the landscape of the Ozark Plateau today look so "young"? Is uplift still taking place, and if so, does this uplift represent continuing flexural response to erosion, or does it imply that a different uplift driver is acting? Second, unlike other FIPs, the Ozark Plateau displays two high areas, the Boston Mountains to the south (the focus of our study) and the St. Francois Mountains on the northeast. The St. Francois Mountains are not explained by our model, so why did they form? To address the first question, we note that as topography evolves, uplift, tilting, and differential erosion drives a reorganization of drainage networks. Because of this reorganization, river profiles do not achieve equilibrium over long timescales (Beeson et al., 2017), even after the flexural response of lithosphere to unloading has concluded. In addition, feedbacks develop in the landscape-evolution system, in that as major rivers form, they can cause changes in base level that can continue to drive local differential erosion to maintain the distinct boundaries of the FIP. To address the second question, we note that the occurrence of the St. Francois Mountains may reflect a flexural response to erosion along the Missouri and Mississippi Rivers, the two largest rivers of North America, which delineate the northeast corner of the Ozark Plateau. This flexure would have been in a direction orthogonal to the direction of flexure in our simplified model. The fact that the edge of the Ozark Plateau, overall, is sharp on the three sides where major rivers flow, but gradual on the west side where no major river exists supports this speculation. Alternatively, the anomalous height of the northeast corner may be related to the structure of the Ozark Dome, in that the area's height may reflect unique crustal characteristics (thickness and/or density) controlling the architecture of the dome so that the area was high to start with. Alternatively, its height may reflect tectonic movements in the two active seismic belts along its borders, or may have developed because basement exposed in the core of the St. Francois Mountains is about 10%–15% denser than limestone and sandstone so erosion of the granite may lead to preferential uplift of the basement rocks, relative to their surroundings (a mechanism suggested by Braun et al., 2014).

The model that we have presented in this paper to explain post-Paleozoic uplift of the Ozark Plateau and its southern escarpment also applies to the other FIPs in the eastern United States. Specifically, the model implies that Deep Valleys Province of the Appalachian Plateau formed due to the erosion of the widest and, presumably, once thickest part of the Valley and Ridge fold-thrust belt, namely, the Pennsylvania salient. This correlation can explain why, as the fold-thrust belt narrows near the endpoints of the salient, the height of the plateau diminishes. Similarly, the Catskill Mountains became defined as a particularly high FIP due to the erosion of the Hudson Valley fold-thrust belt and the western thrust sheets of the Taconic Mountains (erosion that may also have contributed to uplift of the Adirondack Mountains to the north), and the Cumberland Plateau became delineated where a wide portion of the adjacent southern Appalachian fold-thrust belt eroded. Overall, the Appalachian Plateau is lower in elevation adjacent to where it is not bordered by a deeply eroded fold-thrust belt, again suggesting a connection between Plateau elevation and extent of exhumation of the fold-thrust belt. As noted earlier, other causes of uplift likely affect topography in the eastern United States. These causes may play a role in determining the height that FIPs of the eastern United States eventually attained.

6. Conclusions

Foreland intracratonic plateaus (FIPs) are elevated areas underlain by undeformed (nearly flat-lying) cratonic platform and, in places, foreland-basin strata that lie on the cratonic side of a now-inactive fold-thrust belts that formed along the Appalachian-Ouachita orogen. We identify four FIPs in the eastern United States—the Ozark Plateau, the Deep Valleys Province, the Cumberland Plateau, and the Catskill Mountains. In each case, the average elevation of the eroded remnants of the fold-thrust belt are lower than the foreland, and an escarpment delineates the boundary between the fold-thrust belt and the foreland. Because the foreland areas are higher than their surroundings, they are known as plateaus.

The contrast in elevation between FIPs and the adjacent fold-thrust belts indicates that a topographic inversion developed since active thrusting ceased. We propose that the occurrence of FIPs, and of the topographic inversion associated with their formation, can be explained by contrast in resistance to erosion between rocks of fold-thrust belts and rocks of their bordering forelands during the flexural unloading of the region. Fold-thrust belts have lesser resistance to erosion than foreland basins and cratonic platforms due to the higher density of faults and fractures, the greater prevalence of steeply sloping bedding planes to facilitate failure, and the limited spatial scales of influence of hard layers in steeply sloping units. As the fold-thrust belt preferentially erodes, it eventually becomes lower than the undeformed foreland basin, resulting in an escarpment separating the foreland from the fold-thrust belt. We are not the first to propose that there are systematic differences in resistance to erosion that can be related to tectonic or geomorphic settings. For example, Zondervan et al. (2020) document the influence of systematic differences in rock strength among crystalline basement, metamorphosed sedimentary rocks, and unmetamorphosed sedimentary cover on erosion rates and drainage-divide mobility in the High Atlas Mountains.

To test our hypothesis that differences in resistance to erosion lead to the production of FIPs we apply a numerical model (*Landlab*) to the post-orogenic evolution of a fold-thrust belt and foreland with a scale chosen to match that of the Ouachita Mountains/Ozark Plateau region. We find that using only moderate contrasts in rock hardness between the fold-thrust belt and foreland rocks (a factor of 2 to a factor of 10), and an effective elastic thickness of the lithosphere of a few tens of kilometers, we can produce the observed large-scale morphology of the region, characterized by a generally low elevation fold-thrust belt and high FIP with a steep escarpment edge along the proximal edge of the basin, an asymmetric drainage divide within the FIP, and a river following the boundary between the foreland basin and the fold-thrust belt. The results of our model imply that FIP formation does not require post-orogenic differential uplift between the fold-thrust belt and the foreland. If other mechanisms drive uplift in the eastern United States, they may amplify the topographic inversion that produces FIPs. Clearly, spatial variability in resistance to erosion, due to both lithology and deformation, is predictably associated with structural settings and that these patterns are crucial in interpreting post-orogenic landforms and landscape evolution.

Data Availability Statement

Python code used to conduct numerical simulations presented here is available at doi:10.5281/zenodo.5767093. The *Landlab* model platform is available at doi:10.5281/zenodo.3772136. Data used to produce Figure 5c are available at https://doi.org/10.3133/ds1052.

Acknowledgments
We thank Trish Gregg, Yan Zhan, and Brooke Dykstra for discussion of flexure and the tectonic context of the Ozark Plateau. We also benefitted from conversations with Willy Guenther, Mike DeLucia, Jeffrey Kwang, and Evan Thaler on the geology and geomorphology of the Ozarks. We are grateful to an insightful review of an early version of this paper by Lijun Liu. We thank Amanda Keen-Zebert and Mark Hudson for extremely constructive and thoughtful reviews that led us to refine and improve this work.

References

Al Asadi, F., Abdulnaby, W., & Zachry, D. (2017). Subsurface structural analysis using well logs to study faults of the lower Atoka Formation in the Arkoma Basin, northcentral Arkansas. *IOSR Journal of Environmental Science, Toxicology and Food Technology*, *11*(5), 65–77.

Allmendinger, R. W., Jordan, T. E., Kay, S. M., & Isacks, B. L. (1997). The evolution of the Altiplano-Puna plateau of the central Andes. *Annual Review of Earth and Planetary Sciences*, *25*(1), 139–174. https://doi.org/10.1146/annurev.earth.25.1.139

Anthony, D. M., & Granger, D. E. (2007). An empirical stream power formulation for knickpoint retreat in Appalachian Plateau fluviokarst. *Journal of Hydrology*, *343*(3–4), 117–126. https://doi.org/10.1016/j.jhydrol.2007.06.013

Arbenz, J. K. (1989a). The Ouachita system. In A. W.Balley, & A. R.Palmer (Eds.), *The geology of North America—An overview: The geology of North America* (Vol. A, pp. 371–396). Geological Society of America.

Arbenz, J. K. (1989b). Ouachita thrust belt and Arkoma Basin. In R. D. Hatcher, Jr., W. A. Thomas, & G. W.Viele (Eds.), *The Appalachian-Ouachita orogen in the United States: The geology of North America* (Vol. F-2, pp. 621–634). Geological Society of America.

Arbenz, J. K. (2008). Structural framework of the Ouachita Mountains. In N. H.Suneson (Ed.), *Stratigraphic and structural evolution of the Ouachita Mountains and Arkoma Basin, southeastern Oklahoma and west-central Arkansas: Applications to petroleum exploration: 2004 field symposium, circular 112A* (pp. 1–40). Oklahoma Geological Survey.

Arne, D. C. (1992). Evidence from apatite fission-track analysis for regional cretaceous cooling in the Ouachita Mountain fold belt and Arkoma Basin of Arkansas. *American Association of Petroleum Geologists Bulletin*, *76*, 392–402. https://doi.org/10.1306/bdff8812-1718-11d7-8645000102c1865d

Arne, D. C., Green, P. F., & Duddy, I. R. (1990). Thermochronologic constraints on the timing of Mississippi Valley-type ore formation from apatite fission track analysis. *International Journal of Radiation Applications and Instrumentation—Part D: Nuclear Tracks and Radiation Measurements*, *17*(3), 319–323. https://doi.org/10.1016/1359-0189(90)90053-z

Baker, C. (2013). *A model for predicting bedrock failure in the Arkansas River Valley Region of Western Arkansas* (p. 38). Arkansas Geological Survey Miscellaneous Publication 24.

Barnhart, K. R., Hutton, E. W. H., Tucker, G. E., Gasparini, N. M., Istanbulluoglu, E., Hobley, D. E. J., et al. (2020). Short communication: Landlab v2.0: A software package for Earth surface dynamics. *Earth Surface Dynamics*, *8*, 379–397. https://doi.org/10.5194/esurf-8-379-2020

Beaumont, C. (1981). Foreland basins. *Geophysical Journal of the Royal Astronomical Society*, *65*, 291–329. https://doi.org/10.1111/j.1365-246x.1981.tb02715.x

Beaumont, C., Keen, C. E., & Boutilier, R. (1982). A comparison of foreland and rift margin sedimentary basins. *Philosophical Transactions of the Royal Society of London A*, *305*, 295–317.

Beeson, H. W., McCoy, S. W., & Keen-Zebert, A. (2017). Geometric disequilibrium of river basins produces long-lived transient landscapes. *Earth and Planetary Science Letters*, *475*, 34–43. https://doi.org/10.1016/j.epsl.2017.07.010

Bethke, C. M., & Marshak, S. (1990). Brine migrations across North America—The plate tectonics of groundwater. *Annual Review of Earth and Planetary Sciences*, *18*, 287–315. https://doi.org/10.1146/annurev.ea.18.050190.001443

Blackmer, G. C., Omar, G. I., & Gold, D. P. (1994). Post-Alleghanian unroofing history of the Appalachian Basin, Pennsylvania, from apatite fission track analysis and thermal models. *Tectonics*, *13*, 1259–1276. https://doi.org/10.1029/94tc01507

Braun, J., Simon-Labric, T., Murray, K. E., & Reiners, P. W. (2014). Topographic relief driven by variations in surface rock density. *Nature Geoscience*, *7*(7), 534–540. https://doi.org/10.1038/ngeo2171

Bretz, J. H. (1965). *Geomorphic history of the Ozarks of Missouri* (Vol. 41, p. 147). State of Missouri, Department of Business and Administration, Division of Geological Survey and Water Resources.

Brown, S. (2005). *Ozark Plateau, Midcontinental North America: Insights into thermochronology using apatite fission-track analysis* (p. 137) (M.S. thesis, University of Illinois at Urbana-Champaign).

Byrnes, J. S., Bezada, M., Long, M. D., & Benoit, M. H. (2019). Thin lithosphere beneath the central Appalachian Mountains. Constraints from seismic attenuation beneath the MAGIC array. *Earth and Planetary Science Letters*, *519*, 297–307. https://doi.org/10.1016/j.epsl.2019.04.045

Chu, R., Leng, W., Helmberger, D. V., & Gurnis, M. (2013). Hidden hotspot track beneath the eastern United States. *Nature Geoscience*, *6*, 963–966. https://doi.org/10.1038/ngeo1949

Corrigan, J., Cervany, P. F., Donelick, R., & Bergman, S. C. (1998). Postorogenic denudation along the late Paleozoic Ouachita trend, south central United States of America: Magnitude and timing constraints from apatite fission track data. *Tectonics*, *17*, 587–603. https://doi.org/10.1029/98tc01316

Cox, R. T. (1988). Evidence of quaternay ground tilting associated with the Reelfoot rift zone, northeast Arkansas. *Southeastern Geology*, *28*(4), 221–224.

Cox, R. T. (2009). Ouachita, Appalachian and Ancestral Rockies deformations recorded in mesoscale structures on the foreland Ozark plateaus. *Tectonophysics*, *474*(3–4), 674–683. https://doi.org/10.1016/j.tecto.2009.05.005

Cox, R. T., & Van Arsdale, R. B. (2002). The Mississippi Embayment, North America: A first order continental structure generated by the Cretaceous superplume mantle event. *Journal of Geodynamics*, *34*, 163–176. https://doi.org/10.1016/s0264-3707(02)00019-4

Crough, S. T. (1981). Mesozoic hotspot epeirogeny in eastern North America. *Geology*, *9*, 2–6. https://doi.org/10.1130/0091-7613(1981)9<2:mheien>2.0.co;2

Crowley, K. D. (1991). Thermal history of Michigan Basin and Southern Canadian Shield from apatite fission track analysis. *Journal of Geophysical Research: Solid Earth*, *96*(B1), 697–711. https://doi.org/10.1029/90jb02174

Culling, W. (1963). Soil creep and the development of hillside slopes. *The Journal of Geology*, *71*, 127–161. https://doi.org/10.1086/626891

Davis, W. M. (1882). The little mountains east of the Catskills. Appalachia. *The Journal of the Appalachian Mountain Club*, *3*, 20–33.

DeCelles, P. G. (2012). Foreland basin systems revisited: Variations in response to tectonic settings. In C.Busby, & A. A.Pérez (Eds.), *Tectonics of sedimentary basins* (pp. 405–426). Blackwell Ltd. https://doi.org/10.1002/9781444347166.ch20

DeCelles, P. G., & Giles, K. A. (1996). Foreland basin systems. *Basin Research*, *8*, 105–123. https://doi.org/10.1046/j.1365-2117.1996.01491.x

DeLucia, M. S., Guenthner, W. R., Marshak, S., Thomson, S. N., & Ault, A. K. (2018). Thermochronology links denudation of the Great Unconformity surface to the supercontinent cycle and snowball Earth. *Geology*, *46*, 167–170. https://doi.org/10.1130/g39525.1

Dühnforth, M., Anderson, R. S., Ward, D., & Stock, G. M. (2010). Bedrock fracture control of glacial erosion processes and rates. *Geology*, *38*, 423–426.

England, P. C., & Houseman, G. A. (1988). The mechanics of the Tibetan Plateau. *Philosophical Transactions of the Royal Society of London A*, *326*, 301–320.

Flowers, R. M., Ault, A. K., Kelley, S. A., Zhang, N., & Zhong, S. J. (2012). Epeirogeny or eustasy? Paleozoic-mesozoic vertical motion of the North American continental interior from thermochronometry and implications for mantle dynamics. *Earth and Planetary Science Letters*, *317*, 436–445. https://doi.org/10.1016/j.epsl.2011.11.015

Goode, J. R., & Wohl, E. E. (2010). Substrate controls on the longitudinal profile of bedrock channels: Implications for reach-scale roughness. *Journal of Geophysical Research*, *115*. https://doi.org/10.1029/2008JF001188.F03018

Haley, B. R., Glick, E. E., Bush, W. V., Clardy, B. F., Stone, C. G., Woodward, B., & Zachry, D. L. (1993) *Geologic map of Arkansas*. Arkansas Geological Survery and U.S. Geological Survey.

Ham, W. E., & Wilson, J. L. (1967). Paleozoic epeirogeny and orogeny in the central United States. *American Journal of Science*, *265*, 332–407. https://doi.org/10.2475/ajs.265.5.332

Hancock, G. S., Anderson, R. S., Whipple, K. X., Tinkler, K. J., & Wohl, E. E. (1998), *Beyond power: Bedrock river incision process and form* (Vol. 107, pp. 35–60). Geophysical Monograph-American Geophysical Union. https://doi.org/10.1029/gm107p0035

Hobley, D. E. J., Adams, J. M., Nudurupati, S. S., Hutton, E. W. H., Gasparini, N. M., Istanbulluoglu, E., & Tucker, G. E. (2017). Creative computing with Landlab: An open-source toolkit for building, coupling and exploring tow-dimensional numerical models of Earth-surface dynamics. *Earth Surface Dynamics*, *5*, 21–46. https://doi.org/10.5194/esurf-5-21-2017

Hooyer, T. S., Cohen, D., & Iverson, N. R. (2012). Control of glacial quarrying by bedrock joints. *Geomorphology*, *152–154*, 91–101. https://doi.org/10.1016/j.geomorph.2012.02.012

Horton, J. D., San Juan, C. A., & Stoeser, D. B. (2017). *The State Geologic Map Compilation (SGMC) geodatabase of the conterminous United States (ver 1.1, August 2017)* (p. 46). U.S. Geological Survey Data Series 1052. https://doi.org/10.3133/ds1052

Hosseini, M., & Shirin, D. (2015). An estimate of the tensile strength based on P-wave velocity and Schmidt hardness rebound number. *International Journal of Geography and Geology*, *4*(2), 24–36.

Houseknecht, D. W. (1983). *Tectonic-sedimentary evolution of the Arkoma Basin* (Vol. 1, p. 119). Society of Economic Paleontologists and Mineralogists Midcontinent Section.

Houseknecht, D. W. (1986). Evolution from passive margin to foreland basin: The Atoka Formation of the Arkoma Basin, south-central U.S.A. In P. A.Allen, & P.Homewood (Eds.), *Foreland basins* (Vol. 8, pp. 327–345). International Association of Sedimentologists Special Publication.

Houseknecht, D. W., Rouse, W. A., Mars, J. C., Fulk, B., & Paxton, S. T. (2014). Upper Devonian-Mississippian stratigraphic framework of the Arkoma Basin and distribution of potential source-rock facies in the Woodford-Chattanooga and Fayettevill-Caney shale-gas systems. *American Association of Petroleum Geologists Bulletin*, *98*, 1739–1759. https://doi.org/10.1306/03031413025

Hrubcová, P., Geissler, W. H., Bräuer, K., Vavrycuk, V., Tomek, C., & Kämpf, H. (2017). Active magmatic underplating in Western Eger Rift, Central Europe. *Tectonics*, *36*, 2846–2862.

Hu, J., Liu, L., Faccenda, M., Zhou, Q., Fischer, K. M., Marshak, S., & Lundstrom, C. (2018). Modification of the Western Gondwana craton by plume-lithosphere interaction. *Nature Geoscience*, *11*, 203–210. https://doi.org/10.1038/s41561-018-0064-1

Hudson, M. R. (2000). Coordinated strike-slip and normal faulting in the southern Ozark dome of northern Arkansas: Deformation in a late Paleozoic foreland. *Geology*, *28*, 511–514. https://doi.org/10.1130/0091-7613(2000)028<0511:cssanf>2.3.co;2

Jamieson, R. A., & Beaumont, C. (1988). Orogeny and metamorphism: A model for deformation and pressure-temperature-time paths with applications to the central and southern Appalachians. *Tectonics*, *7*, 417–445. https://doi.org/10.1029/tc007i003p00417

Keen-Zebert, A. K., Hudson, M., Shepherd, S., & Thaler, E. (2017). The effect of lithology on valley width, terrace distribution, and bedload provenance in a tectonically stable catchment with flat-lying stratigraphy. *Earth Surface Processes and Landforms*, *42*(10), 1573–1587. https://doi.org/10.1002/esp.4116

Kelly, M. H., Anders, A. M., & Gran Mitchell, S. (2014). Influence of bedding dip on glacial erosional landforms, Uinta Mountains, USA. *Geografiska Annaler—Series A: Physical Geography*, *96*, 14–159. https://doi.org/10.1111/geoa.12037

Krabbendam, M., & Glasser, N. F. (2011). Glacial erosion and bedrock properties in NW Scotland: Abrasion and plucking, hardness and joint spacing. *Geomorphology*, *130*, 374–383. https://doi.org/10.1016/j.geomorph.2011.04.022

Lamb, M. P., Finnegan, N. J., Scheingross, J. S., & Sklar, L. (2015). New insights into the mechanics of fluvial bedrock erosion through flume experiments and theory. *Geomorphology*, *244*, 33–55. https://doi.org/10.1016/j.geomorph.2015.03.003

Levander, A., Schmandt, B., Miller, M. S., Liu, K., Karlstrom, K. E., Crow, R. S., et al. (2011). Continuing Colorado plateau uplift by delamination-style convective lithospheric downwelling. *Nature*, *472*, 461–465. https://doi.org/10.1038/nature10001

Levine, J. R. (1986). Deep burial of coal-bearing strata, Anthracite region, Pennsylvania: Sedimentation or tectonics? *Geology*, *14*, 577–580. https://doi.org/10.1130/0091-7613(1986)14<577:dbocsa>2.0.co;2

Lin, L., Gao, S. S., Liu, K. H., & Mickus, K. (2017). Receiver function and gravity constraints on crustal structure and vertical movements of the Upper Mississippi Embayment and Ozark Uplift. *Journal of Geological Research*, *122*, 4572–4583. https://doi.org/10.1002/2017JB014201

Liu, L. (2014). Rejuvenation of Appalachian topography caused by subsidence-induced differential erosion. *Nature Geoscience*, *7*, 518–523. https://doi.org/10.1038/ngeo2187

Liu, L. (2015). The ups and downs of North America: Evaluating the role of mantle dynamic topography since the Mesozoic. *Reviews of Geophysics*, *53*, 1022–1049. https://doi.org/10.1002/2015RG000489

Liu, L., & Gurnis, M. (2010). Dynamic subsidence and uplift of the Colorado Plateau. *Geology*, *38*(7), 663–666. https://doi.org/10.1130/g30624.1

Long, W. A. (2005). The Mulberry Fault zone: An analysis of subsurface geometry and timing of fault displacement (*M.S. thesis*, University of Arkansas, Fayetteville).

Lovell, T. R. (2017). *An intracratonic record of North American tectonics (Doctoral dissertation)*. Purdue University. Retrieved from ProQuest, 10602462.

Mariño, J., Marshak, S., & Mastalerz, M. (2015). Evidence for stratigraphically controlled paleogeotherms in the Illinois Basin based on vitrinite-reflectance analysis: Implications for interpreting coal-rank anomalies. *American Association of Petroleum Geologists Bulletin*, *99*, 1803–1825.

Marshak, S. (1986). Structure and tectonics of the Hudson Valley fold-thrust belt, New York. *The Geological Society of America Bulletin*, *97*, 354–368. https://doi.org/10.1130/0016-7606(1986)97<354:satoth>2.0.co;2

Marshak, S., & Paulsen, T. (1996). Midcontinent US fault and fold zones: A legacy of Proterozoic intracratonic extensional tectonism. *Geology*, *24*, 151–154. https://doi.org/10.1130/0091-7613(1996)024<0151:musfaf>2.3.co;2

Marshak, S., & van der Pluijm, B. A. (2021). Tectonics of the continental interior in the United States. In D.Alderton, & S. A.Elias (Eds.), *Encyclopedia of geology* (2nd ed., Vol. 4, pp. 173–186). Academic Press. https://doi.org/10.1016/b978-0-08-102908-4.00139-9

Marshall, J. A., & Roering, J. J. (2014). Diagenetic variation in the Oregon Coast Range: Implications for rock strength, soil production, hillslope form, and landscape evolution. *Journal of Geophysical Research: Earth Surface*, *199*, 1395–1417. https://doi.org/10.1002/2013JF003004

Matmon, A., Bierman, P. R., Larsen, J., Southworth, S., Pavich, M., & Caffee, M. (2003). Temporally and spatially uniform rates of erosion in the Southern Appalachian Great Smoky Mountains. *Geology*, *31*(2), 155–158. https://doi.org/10.1130/0091-7613(2003)031<0155:tasuro>2.0.co;2

McCracken, M. H. (1971). *Structural features of Missouri. Report of investigations* (Vol. 49, pp. 1–99), Missouri Geological Survey.

McKeon, R. E., Zeitler, P. K., Pazzaglia, F. J., Idleman, B. D., & Enkelmann, E. (2014). Decay of an old orogen: Inferences about Appalachian landscape evolution from low-temperature thermochronology. *Geological Society of America Bulletin*, *126*, 31–46. https://doi.org/10.1130/b30808.1

McKeown, F. A., Jones-Cecil, M., Askew, B. L., & McGrath, M. B. (1988). *Analysis of stream-profile data and inferred tectonic activity, Eastern Ozark Mountains Region*. US Geological Survey Bulletin 1807.

Miller, D. S., & Duddy, I. R. (1989). Early Cretaceous uplift and erosion of the northern Appalachian Basin, New York, based on apatite fission track analysis. *Earth and Planetary Science Letters*, *93*(1), 35–49.

Miller, J. R. (1990). The influence of bedrock geology on knickpoint development and channel-bed degradation along downcutting streams in south-central Indiana. *The Journal of Geology*, *99*, 591–605.

Miller, S. R., Sak, P. B., Kirby, E., & Bierman, P. R. (2013). Neogene rejuvenation of central Appalachian topography: Evidence for differential rock uplift from stream profiles and erosion rates. *Earth and Planetary Science Letters*, *369*(370), 1–12.

Moucha, R., Forte, A. M., Mitrovica, J. X., Rowley, D. B., Quéré, S., Simmons, N. A., & Grand, S. P. (2008). Dynamic topography and long-term sea-level variations: There is no such thing as a stable continental platform. *Earth and Planetary Science Letters*, *271*, 101–108.

Murphy, B. S., & Egbert, G. D. (2017). Electrical conductivity structure of southeastern North America: Implication for lithospheric architecture and Appalachian topographic rejuvenation. *Earth and Planetary Science Letters*, *462*, 66–75. https://doi.org/10.1016/j.epsl.2017.01.009

Nasseri, M. H., Rao, K. S., & Ramamurth, T. (1997). Failure mechanism in schistose rocks. International. *Journal of Rock Mechanics and Mining Sciences*, *34*, 219e1–219e15. https://doi.org/10.1016/S1365-1609(97)00099-3

Nelson, W. J. (1995). *Structural features in Illinois*. Illinois State Geological Survey Bulletin No. 100.

Northcutt, R. A., & Campbell, J. A. (1995). Geologic provinces of Oklahoma. In J. P. Hogan, & M. C. Gilbert (Eds.), *Basement tectonics 12* (Vol. 6, pp. 29–37).

Nyblade, A. A., & Sleep, N. H. (2003). Long lasting epeirogenic uplift from mantle plumes and the origin of the Southern African Plateau. *Geochemisty, Geophysics, Geosystems*, *4*(12). https://doi.org/10.1029/2003GC000573

O'Callaghan, J. F., & Mark, D. M. (1984). The extraction of drainage networks from digital elevation data. *Computer Vision, Graphics, and Image Processing*, *28*, 323–344.

Oliver, J. (1986). Fluids expelled tectonically from orogenic belts, their role in hydrocarbon migration and other geological phenomena. *Geology*, *14*, 99–102.

Oskin, M. E., Burbank, D. W., Phillips, F. W., Marrero, S. M., Bookhagen, B., & Selander, J. A. (2014). Relationship of channel steepness to channel incision rate from a tilted and progressively exposed unconformity surface. *Journal of Geophysical Research: Earth Surface*, *199*. https://doi.org/10.1002/2013.JF002826

Pazzaglia, F. J., & Gardner, T. W. (2000). Late Cenozoic landscape evolution of the US Atlantic passive margin: Insights into a North American Great Escarpment. In M. A.Summerfield (Ed.), *Geomorphology and global tectonics* (pp. 283–302). John Wiley & Sons.

Peppers, M. H. (2015). Unraveling controls on fracture stratigraphy in carbonates: The influence of regional stress, mechanical properties, and diagenesis (Master's thesis). University of Nebraska—Lincoln. Retrieved from Digital Commons http://digitalcommons.unl.edu/geoscidiss/65

Pérez-Peña, J. V., Al-Awabdeh, M., Azañón, J. M., Galve, J. P., Booth-Rea, G., & Notti, D. (2017). SwathProfiler and NProfiler: Two new ArcGIS Add-ins for the automatic extraction of swath and normalized river profiles. *Computers & Geosciences*, *104*(135), 150. https://doi.org/10.1016/j.cageo.2016.08.008

Powell, C. M. A. (1986). Continental underplating model for the rise of the Tibetan Plateau. *Earth and Planetary Science Letters*, *81*(1), 79–94.

Price, R. A. (1973). Large-scale gravitational flow of supracrustal rocks, southern Canadian Rockies. In K. A.De Jong, & R.Scholten (Eds.), *Gravity and tectonics* (pp. 491–502). John Wiley & Sons.

Purser, J. L., & Van Arsdale, R. B. (1998). Structure of the Lake County uplift: New Madrid seismic zone. *Bulletin of the Seismological Society of America*, *88*, 1204–1211.

Quinlan, G. M., & Beaumont, C. (1984). Appalachian thrusting, lithospheric flexure, and the Paleozoic stratigraphy of the eastern interior of north-America. *Canadian Journal of Earth Sciences*, *21*, 973–996.

Reminga, K. N., Weber, J. C., & Seong, Y. B. (2016). A preliminary in-situ and basin-wide 10Be TCN Study of the Ste. Francois and Ozark Mountains Landscape. *Geological Society of America Abstracts with Programs*, *48*(7). https://doi.org/10.1130/abs/2016AM-287264

Roden, M. K., & Miller, D. S. (1989). Apatite fission-track thermochronology of the Pennsylvania Appalachian Basin. *Geomorphology*, *2*, 39–51.

Ruetenik, G., & Moucha, R. (2021). Escarpment retreat on a viscoelastic lithosphere. In *EGU General Assembly 2021, online, 19–30 Apr 2021, EGU21-12331*, https://doi.org/10.5194/egusphere-egu21-12331

Scott, D. N., & Wohl, E. E. (2019). Bedrock fracture influences on geomorphic process and form across process domains and scales. *Earth Surface Processes and Landforms*, *44*(1), 27–45.

Selby, M. J. (1982). *Hillslope materials and processes*. Oxford University Press.

Sklar, L., & Dietrich, W. E. (2001). Sediment and rock strength controls on river incision into bedrock. *Geology*, *29*, 1087–1090.

Spotila, J. A., Bank, G. C., Reiners, P. W., Naeser, C. W., Naeser, N. D., & Henika, B. S. (2004). Origin of the Blue Ridge escarpment along the passive margin of Eastern North America. *Basin Research*, *16*, 41–63.

Sutherland, P. K. (1988). Late Mississippian and Pennsylvanian depositional history in the Arkoma basin area, Oklahoma and Arkansas. *The Geological Society of America Bulletin*, *100*, 1787–1802.

Swanson, C. D. (2016). Exploring the controls of bedrock characteristics on channel form: Ouachita Mountains, *Arkansas (Master's thesis)*. Tulane University School of Science and Engineering. Retrieved from ProQuest, 10192757 https://www.proquest.com/docview/1887970487?pq-origsite=gscholar&fromopenview=trueNewOrleans

Thaler, E. A., & Covington, M. D. (2016). The influence of sandstone caprock material on bedrock channel steepness within a tectonically passive setting: Buffalo National River Basin, Arkansas, USA. *Journal of Geophysical Research: Earth Science*, *121*, 1635–1650. https://doi.org/10.1002/2015JF003771

Thomas, W. A. (1976). Evolution of Ouachita-Appalachian continental margin. *The Journal of Geology*, *84*, 323–342.

Thomas, W. A. (2011). The Iapetan rifted margin of southern Laurentia. *Geosphere*, *7*, 97–120.

Thompson Jobe, J. A., Gold, R. D., Briggs, R. W., Williams, R. A., Stephenson, W. J., Delano, J. E., et al. (2020). Evidence for late Quaternary deformation along Crowleys Ridge, New Madrid seismic Zone. *Tectonics*, *39*, e2019TC005746. https://doi.org/10.1029/2019TC005746

Turcotte, D. L., & Schubert, G. (2002). *Geodynamics* (2nd ed.). Cambridge University Press.

Van Arsdale, R. B., Williams, R. A., Schweig, E. S., Shedlock, K. M., Odum, J. K., & Kink, K. W. (1995). The origin of Crowley's Ridge, northeastern Arkansas: Erosional remnant or tectonic uplift? *Bulletin of the Seismological Society of America*, *85*, 963–985.

van der Lee, S., Regenauer-Lieb, K., & Yuan, D. A. (2008). The role of water in connecting past and future episodes of subduction. *Earth and Planetary Science Letters*, *273*, 15–27. https://doi.org/10.1016/j.epsl.2008.04.041

Viele, G., & Thomas, W. A. (1989). Tectonic synthesis of the Ouachita orogenic belt. In R. D. Hatcher, Jr., W. A. Thomas, & G. W. Viele, (Eds.), *The Appalachian-Ouachita orogen in the United States the Geology of North America* (Vol. F-2, pp. 695–728). The Geological Society of America.

Viele, G. W. (1973). Structure and tectonic history of the Ouachita Mountains, Arkansas. In K. A.De Jong, & R.Scholten (Eds.), *Gravity and tectonics* (pp. 361–377). John Wiley & Sons.

Waschbusch, J., & Royden, L. H. (1992). Spatial and temporal evolution of foredeep basins: Lateral strength variations and inelastic yielding in continental lithosphere. *Basin Research*, *4*, 179–196.

White, R., & McKenzie, D. (1989). Magmatism at rift zones: The generation of volcanic continental margins and flood basalts. *Journal of Geophysical Research*, *94*, 7685–7729.

Wickert, A. D. (2016). Open-source modular solutions for flexural isostasy: GFlex v1.0. *Geoscientific Model Development*, *9*, 997–1017. https://doi.org/10.5194/gmd-9-997-2016

Winkler, S., & Matthews, J. A. (2014). Comparison of electronic and mechanical Schmidt hammers in the context of exposure-age dating: Are Q- and R-values interconvertible? *Earth Surface Processes and Landforms*, *39*(8), 1128–1136.

Wylie, D. C., & Mah, C. W. (2001). *Rock slope engineering: Civil and mining*. Spoon Press.

Yang, X., Pavlis, G. L., Hamburger, M. W., Sherrill, E., Gilbert, H., Marshak, S., et al. (2014). Seismicity of the Ste. Genevieve seismic zone based on observations from the EartScope OIINK Flexible array. *Seismological Research Letters*, *85*(6), 1285–1294.

Zhang, N., Zhong, S., & Flowers, R. M. (2012). Predicting and testing continental vertical motion histories since the Paleozoic. *Earth and Planetary Science Letters*, *317*(318), 426–435.

Zondervan, J. R., Stokes, M., Boulton, S. J., Tefler, M. W., & Mather, A. E. (2020). Rock strength and structural controls on fluvial erodibility: Implications for drainage divide mobility in a collisional mountain belt. *Earth and Planetary Science Letters*, *538*, 116221.